WL-TR-94-4080

LIFE PREDICTION METHODOLOGY FOR COMPOSITE LAMINATES
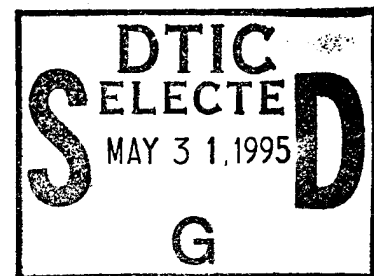
PART II: SPECTRUM FATIGUE

JEFFERY R. SCHAFF

BARRY D. DAVIDSON
DEPT OF MECHANICAL, AEROSPACE, AND MANUFACTURING ENGINEERING
SYRACUSE UNIVERSITY
SYRACUSE NEW YORK

DECEMBER 1994

APPROVED FOR PUBLIC RELEASE; DISTRIBUTION IS UNLIMITED
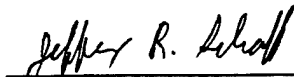
DTIC
SELECTED
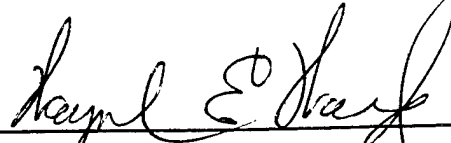MAY 3 1,1995
G

19950530 070

NOTICE

When Government drawings, specifications, or other data are used for any purpose other than in connection with a definitely Government-related procurement, the United States Government incurs no responsibility or any obligation whatsoever. The fact that the government may have formulated or in any way supplied the said drawings, specifications, or other data, is not to be regarded by implication, or otherwise in any manner construed, as licensing the holder, or any other person or corporation; or as conveying any rights or permission to manufacture, use, or sell any patented invention that may in any way be related thereto.

This report is releasable to the National Technical Information Service (NTIS). At NTIS, it will be available to the general public, including foreign nations.
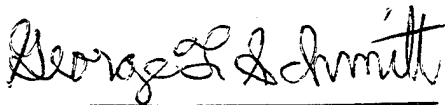
This technical report has been reviewed and is approved for publication.

JEFFERY R. SCHAFF, 1Lt, USAF
Materials Research Engineer
Mechanics & Surface Interactions Br

WAYNE E. WARD, Acting Chief
Mechanics & Surface Interactions Br
Nonmetallic Materials Division

GEORGE F. SCHMITT
Assistant Chief
Nonmetallic Materials Division
Materials Directorate

If your address has changed, if you wish to be removed from our mailing list, or if the addressee is no longer employed by your organization please notify WL/MLBM , WPAFB, OH 45433-7750 to help us maintain a current mailing list.

Copies of this report should not be returned unless return is required by security considerations, contractual obligations, or notice on a specific document.

REPORT DOCUMENTATION PAGE

1. AGENCY USE ONLY *(Leave blank)*	2. REPORT DATE	3. REPORT TYPE AND DATES COVERED
	December 1994	INTERIM 15 Jan 93 - 30 Dec 94

4. TITLE AND SUBTITLE

LIFE PREDICTION METHODOLOGY FOR COMPOSITE LAMINATES
PART II: SPECTRUM FATIGUE

6. AUTHOR(S)

JEFFERY R. SCHAFF
BARRY D. DAVIDSON

5. FUNDING NUMBERS

C: -----
PE: 62102
PR: 2419
TA: 03
WU: 10

7. PERFORMING ORGANIZATION NAMES(S) AND ADDRESS(ES)

MATERIALS DIRECTORATE
WRIGHT LABORATORY
AIR FORCE MATERIEL COMMAND
WRIGHT-PATTERSON AFB OH 45433-7734

8. PERFORMING ORGANIZATION REPORT NUMBER

9. SPONSORING / MONITORING AGENCY NAME(S) AND ADDRESS(ES)

MATERIALS DIRECTORATE
WRIGHT LABORATORY
AIR FORCE MATERIEL COMMAND
WRIGHT-PATTERSON AFB OH 45433-7734

10. SPONSORING / MONITORING AGENCY REPORT NUMBER

WL-TR-94-4080

11. SUPPLEMENTARY NOTES

13. ABSTRACT *(Maximum 200 words)*

A previously developed model for predicting the life of composite structures under constant amplitude and two-stress level fatigue loadings is extended and applied to structures subjected to randomly-ordered loading spectra. The model is phenomenological and a limited amount of experimental data is required for its characterization. For uniaxially loaded laminates, this consists of static tension and compression strength distributions, S-N curves based on constant amplitude fatigue life distributions for two-to-three stress ratios, and a limited amount of two-stress level fatigue test results. The model is verified by comparing predicted fatigue life distributions to experimentally observed fatigue life data for a variety of laminates and load spectrums. Good correlation between theory and experiment is obtained for all loadings and laminates studied.

14. SUBJECT TERMS
LIFE PREDICTION, FATIGUE, COMPOSITE MATERIALS

15. NUMBER OF PAGES
35

16. PRICE CODE

17. SECURITY CLASSIFICATION OF REPORT	18. SECURITY CLASSIFICATION OF THIS PAGE	19. SECURITY CLASSIFICATION OF ABSTRACT	20. LIMITATION OF ABSTRACT
UNCLASSIFIED	UNCLASSIFIED	UNCLASSIFIED	UL

TABLE OF CONTENTS

LIST OF FIGURES

1. INTRODUCTION

In Part I of this work (Schaff and Davidson, 1994a), a "strength-based wearout" model was developed for predicting the life of composite structures subjected to constant amplitude and two-stress level fatigue loadings. This model is phenomenological and experimental results from monotonic and a limited number of cyclic tests are required for the determination of certain model parameters. For the relatively simple loadings considered in Part I, the cyclic tests necessary to characterize the model were assumed to be performed at each load amplitude of interest. However, many practical load histories contain numerous stress levels, and to use experimental data to characterize the model at each of these would necessitate an extremely large number of tests.

In what follows, the model described in Part I is extended and applied to predict fatigue life distributions for composite structures subjected to randomly-ordered load spectra. As in Part I, the model may be applied to any structural configuration that undergoes proportional cyclic loadings. The principal step in extending the model to spectrum fatigue is the development of a procedure to obtain all of the model's parameters for each stress level of the spectrum using only a small amount of experimental input. For structures subjected to a spectrum containing cycles with mean stresses of both signs, this procedure requires experimental determination of the structure's static strength under positive and negative stress, S-N curves at three stress ratios, and a limited amount of two-stress level fatigue test results. To verify the accuracy of the model and the associated model characterization procedures, predicted fatigue life distributions are compared to experimental fatigue life data for three different laminate types subjected to a variety of uniaxial spectrum fatigue loadings. Good correlation is obtained for all cases considered.

2. THEORY

In this section, the model's relationships developed in Part I for a structure's residual strength and probability of failure are generalized to randomly-ordered loadings. The loading spectrum is assumed to be comprised of a series of constant amplitude segments. The number of loading cycles in a given segment is arbitrary, and for certain spectrums may only be on the order of a few cycles. Thus, the "i^{th}" segment is defined as a series of loading cycles, n_i, in which the peak stress and mean stress are constant. At present, it is assumed that the model's parameters that characterize that segment, e.g., the fatigue life scale parameter, N_i, the fatigue life shape parameter, B_{l_i}, and the

1

strength degradation parameter, v_i, are all known. Determination of these parameters from a relatively modest amount of data is addressed in a subsequent section. As in Part I, for multi-axially, proportionately loaded structures, "tension" and "compression" loads are represented in terms of the single parameter that is used to describe the loading.

2.1 Residual Strength

In order to obtain a generalized relation for the residual strength scale parameter from that developed in Part I, we first consider a three-stress level loading sequence. Eq. (12) of Part I gives the scale parameter for residual strength at the end of the first two loading segments. Following the same reasoning, the residual strength scale parameter for the third segment is given by

$$R(n_1+n_2+n_j) = R_o - (R_o-S_3) \left(\frac{n_j+n_{eff_3}}{N_3}\right)^{v_3} \tag{1a}$$

where n_j is the number of cycles elapsed within the third segment, S_3 is the peak stress defining the third segment, and the effective number of cycles for the third segment, n_{eff_3}, is given by

$$n_{eff_3} = N_3 \left(\frac{R_o-R(n_1+n_2)}{R_o-S_3}\right)^{1/v_3} \tag{1b}$$

Here, $R(n_1+n_2)$ is determined using Eq. (12) of Part I. The strength at the end of the third segment is obtained by substituting n_3 for n_j in Eq. (1a).

Generalization of Equations (1a) and (1b) to an arbitrary number of loading segments yields

$$R\left(\sum_{i=1}^{j} n_i\right) = R_o - (R_o-S_j) \left(\frac{n_j+n_{eff_j}}{N_j}\right)^{v_j} \tag{2a}$$

where
$j=$	current segment
$R_o=$	static strength scale parameter
$n_i=$	number of cycles in segment i for $i \neq j$
$n_j=$	number of elapsed cycles in segment j
$v_j=$	strength degradation parameter for segment j
$S_j=$	peak stress defining segment j
$N_j=$	fatigue life distribution scale parameter for segment j

2

The effective number of cycles for the "j^{th}" segment, n_{eff_j}, is defined as

$$n_{eff_j} = N_j \left(\frac{R_o - R\left(\sum\limits_{i=1}^{i-1} n_i\right)}{R_o - S_j} \right)^{1/v_j} \tag{2b}$$

Notice that the residual strength scale parameter at the end of each segment is required in order to obtain the value

for the next segment. Thus, the model must always be applied on a segment-by-segment basis.

2.2 Probability of Failure

The probability of failure during the "j^{th}" loading segment may be expressed as

$$P\left[\hat{R}\left(\sum_{i=1}^{j} n_i\right) \leq S_j\right] = 1 - \exp\left[-\left(\frac{S_j}{R\left(\sum\limits_{i=1}^{j} n_i\right)}\right)^{B_{f_j}(n_j)}\right] \tag{3}$$

where, as in Part I, $\hat{R}$ is used to denote the statistical distribution of strength. $R(\Sigma n_i)$ is given by Equations (2), and $B_{f_j}(n_j)$ is given by Equations (16a) - (16c) of Part I.

As discussed in Part I, the model defines the current probability of failure as the largest probability of failure up

to and including the current load segment.

2.3 Strength Conversion

For structures that experience both tension and compression dominated load cycles, a procedure must be developed

to convert between residual tension and compression strengths. The fundamental issue is the affect of tension-

induced damage on compression strength and vice-versa. Although there are some experimental results which

indicate that cycling under a mean stress of a given sign degrades the residual static strength for loading under the

opposite sign (e.g., Hahn, 1979; Tsai, 1988), their interpretation is made more difficult by coupon-specific failure

modes, such as free edge delamination, that will not occur in full-scale structure. This significantly complicates the

development of an empirically derived quantitative relation. Alternatively, to address this issue using an analytical

or numerical model would require detailed micro-mechanical considerations of the nature and scale of damage in

the structure. This is clearly beyond the scope of the present approach. Rather, we addressed the issue

phenomenologically, with the goal of developing a relation between the strength loss in compression versus that in tension that reasonably reflects observances.

As an example, consider the case where the Weibull scale parameter for static tension strength is significantly larger than that for compression. Further, suppose that a very limited amount of tension dominated cycling occurs and then the loading sense is reversed. Over the first segment, the model predicts residual strength loss in tension; over the second segment, the model must predict the strength loss in compression *from the current state*. Clearly, the compression strength at the beginning of this second segment cannot be equal in magnitude to the residual tension strength, because this may exceed the static compression strength. Alternatively, the experimental evidence cited above indicates that the initial compression strength, at the start of the second segment, is likely lower than the static compression strength. To account for this effect, the model degrades the residual compressive strength by the same percentage as was predicted for tension, and it employs a similar relation for changes from compression to tension dominated cycling. Explicitly, the following relations are used:

$$R^c(n) = R^t(n) \frac{R_o^c}{R_o^t} \qquad (tension \rightarrow compression) \tag{4a}$$

$$R^t(n) = R^c(n) \frac{R_o^t}{R_o^c} \qquad (compression \rightarrow tension) \tag{4b}$$

where R_o^c and R_o^t are the static compression and tension strength scale parameters, respectively.

2.4 Cycle Mix

For spectrum loading, the cycle mix factor is applied during each load transition where the magnitude of the mean stress increases. For loadings that contain sign changes in the mean stress, it is preferable to use two cycle mix constants: one is used for transitions to a compressive mean stress, and a second is used for transitions to a positive mean stress. These constants are obtained from small and large block two-stress level fatigue test results as described in Part I of this work. The effects of cycle mix are most pronounced for those loading spectrums where the number of cycles in any given constant amplitude segment are small.

3. MODEL CHARACTERIZATION FOR GENERAL LOADING SPECTRUMS

In this section, we consider the determination of the fatigue life scale parameters, N_i, the fatigue life shape parameters, B_{l_i}, and the strength degradation parameters, v_i, that are used by the model to characterize each segment of a particular load spectrum. These parameters are obtained from a relatively modest amount of static strength, constant amplitude fatigue, and two-stress level fatigue test data through the use of a series of master diagrams.

3.1 Experimental Database

3.1.1 <u>Monotonic Tests</u>

Monotonic tests are required to determine the structure's static strength and its associated Weibull distribution. If the model is to be used to predict the life of a structure that is subjected to mean stresses of only one sign, a minimum of five tests are required. For example, if only positive mean stresses are included in the spectrum of interest, then the only monotonic test data needed is for failure under positive stress. The data from these tests is reduced by the maximum likelihood method (Talreja, 1981) to obtain the static strength Weibull distribution. For structures subjected to loadings that contain mean stresses of both signs, at least five tension and five compression tests are required to obtain R_0^t, B_s^t, R_0^c and B_s^c, i.e., the scale and shape parameters, respectively, for the static tension and compression strength distributions.

3.1.2 <u>Cyclic Tests</u>

The results of constant amplitude tests are used to determine those model parameters that are necessary to predict the strength degradation during a loading segment, and two-stress level test results are used to determine the one or two required cycle mix constants. Depending upon the loading spectrum of interest, constant amplitude tests are required at either two or three stress ratios. For convenience, denote these ratios as R_{so}, R_{s1} and R_{s2}. In our notation, R_{so} is always used in the test program, R_{s1} is only used when there are load cycles in the spectrum with a positive mean stress, and R_{s2} is only used when there are cycles with a negative mean stress. Thus, *both* R_{s1} and R_{s2} are used only when the loading spectrum contains cycles of both types. These same stress ratios are also used for cycle mix testing. The way in which R_{so}, R_{s1} and R_{s2} are chosen is discussed below, along with the aid of the

5

partial master diagram of Figure 1. This diagram is for a material or structure with equal strengths in tension and compression. It contains no experimental data, but simply plots lines of constant stress ratio versus mean stress and stress amplitude. The conventional definitions of mean stress, S_{mn}, stress amplitude, S_a, and stress ratio, R_s, are adopted, i.e.,

$$S_{mn} = (S_{max} + S_{min}) / 2 \qquad S_a = (S_{max} - S_{min}) / 2 \qquad R_s = S_{min} / S_{max} \tag{5}$$

where S_{max} is the maximum stress defining a segment and S_{min} the minimum stress.

Suppose that the spectrum of interest contains stress ratios only in the range $0 \leq R_s < 1$, denoted in Figure 1 as tension-tension fatigue. With reference to the figure, for spectrums that contain mean stresses of only one sign, R_{so} is always chosen as an "inner bound." In this example, R_{so} would be chosen equal to the smallest stress ratio in the spectrum or else equal to zero. R_{s1} is chosen to "best characterize" the remaining tension dominated loads in the spectrum. It is always at positive mean stress, and will lie on the tension dominated side of the master diagram between R_{so} and $R_s = 1$. Typically, R_{s1} is chosen relatively close to the most commonly occurring tension dominated stress ratio in the spectrum. If the loading spectrum contains stress ratios in the range $-1 \leq R_s < 1$, i.e., tension dominated fatigue, then R_{so} can be chosen equal to the smallest (most negative) stress ratio in the spectrum or else it can be taken equal to -1. R_{s1} is chosen in the same manner as above.

For compression-compression fatigue, all stress ratios are greater than 1.0. Thus, choosing R_{so} as an "inner bound" means it is equal to or greater than the largest stress ratio in the spectrum; $R_{so} = \infty$ is the upper limit for this case. R_{s2} is chosen to "best characterize" the remaining loads in the spectrum. It is always at a negative mean stress and will lie on the compression dominated side of the master diagram between R_{so} and $R_s = 1$. Similar to R_{s1}, R_{s2} is chosen relatively close to the most commonly occurring compression dominated stress ratio in the spectrum. For compression dominated fatigue, e.g., $|R_s| > 1$, R_{so} is chosen equal to -1 or to the largest stress ratio of all compression-tension cycles ($-\infty \leq R_s < -1$) in the spectrum, and the procedure for choosing R_{s2} is unchanged. Finally, for loading spectrums containing mean stresses of both signs, $R_{so} = -1$ is used, R_{s1} is chosen to best characterize the tension dominated cycles, and R_{s2} is chosen to best characterize the compression dominated cycles.

For each stress ratio chosen, individual S-N curves are plotted using Weibull fatigue life scale parameters. To
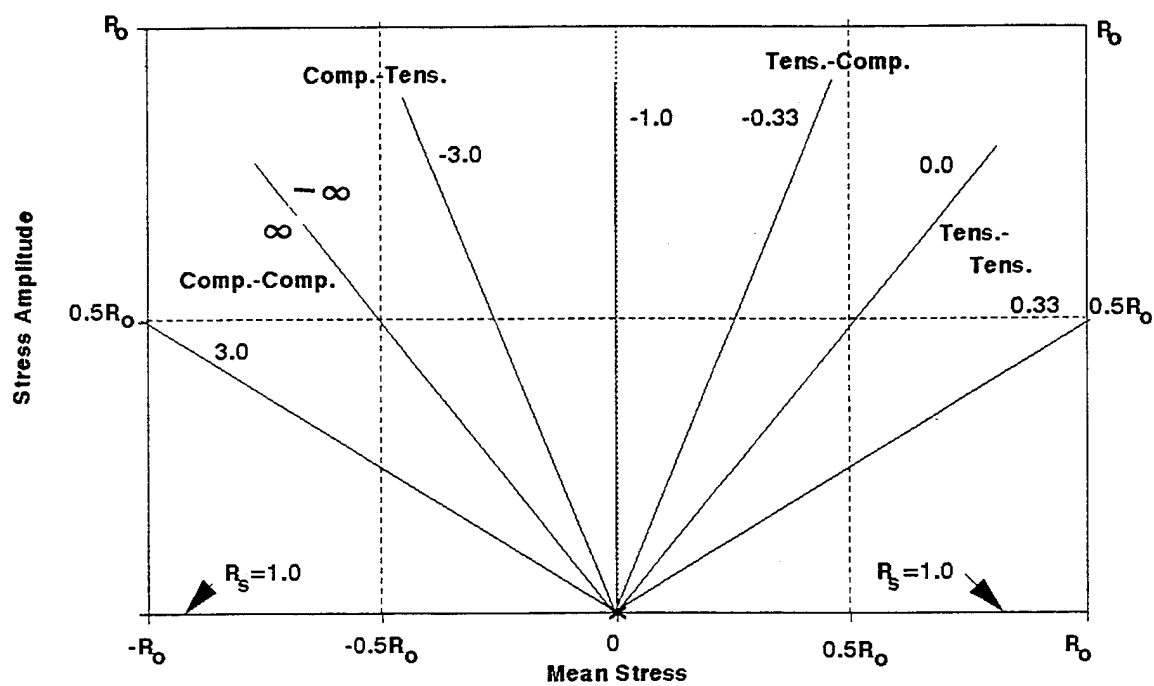
6

Figure 1. Master diagram showing lines of constant stress
ratio. R_0 is the tension and compression strength. Numbers
are values of R_S.

this end, at a given stress ratio, at least five tests are performed at each of three stress amplitudes. Each set of five or more tests are reduced to obtain a fatigue life scale parameter, N, and a fatigue life shape parameter, B_1. The individual S-N curves therefore represent the behavior of the 63.2 percentile of the life distributions.

To determine the one or two cycle mix constants, two-stress level fatigue testing is conducted. The cycle mix constant for transitions to a positive mean stress is obtained by small and large block tension-tension tests at stress ratio R_{s1}, and the cycle mix constant for transitions to a negative mean stress is obtained by small and large block compression-compression testing at stress ratio R_{s2}. The stress amplitudes in these blocks should be typical of those in the loading spectrum of interest.

The type and number of tests that are required to characterize the model for an arbitrary loading spectrum are summarized in Table 1. In the table, "+" refers to a spectrum that contains only tension dominated cycles (positive mean stress), and "-" refers to a spectrum that contains only compression dominated load cycles. We also point out that this table presents the *minimum* number of tests that must be performed for each type of spectrum. More tests are of course preferable, as they provide a more statistically significant sample size.

Table 1. Type and Number of Tests Required for Model Characterization

Type of Test:	Mean Stress in Spectrum		
	"+" only	"-" only	"+" and "-"
Static Tension	5	0	5
Static Compression	0	5	5
S-N curve at Stress Ratio:			
R_{so} (5 replicates at 3 stress amplitudes)	15	15	15
R_{s1} (5 replicates at 3 stress amplitudes)	15	0	15
R_{s2} (5 replicates at 3 stress amplitudes)	0	15	15
Large & Small Block at Stress Ratio:			
R_{s1} (5 tests of each type)	10	0	10
R_{s2} (5 tests of each type)	0	10	10
Total number of tests required:	45	45	75

3.2 Determination of N, B_1 and v for Arbitrary Loadings

For characterization of a structure's behavior under a fully reversed loading spectrum, (i.e., one that contains both positive and negative mean stress), the results of the previous experiments and associated data reduction procedures will provide the static strength scale and shape parameters, the scale and shape parameters for fatigue life for constant amplitude loadings at three stress amplitudes at each of three stress ratios, and the two cycle mix constants. The critical step in model characterization is to generalize these results to provide the key model parameters, N, B_1 and v, for each stress amplitude and stress ratio that occur in the loading spectrum. For the fatigue life scale parameter, N, this is accomplished through a "standard" master diagram (e.g., Tsai, 1988) and modified Goodman relations (Goodman, 1930; Farrow, 1993). Arbitrary values of the fatigue life scale parameter, B_1, and the strength degradation parameter, v, are obtained through "modified" master diagrams.

Consider the construction of a master diagram that will be used to determine the fatigue life, N, corresponding to an arbitrary mean stress and stress amplitude. First, the previously developed S-N curves for the 63.2% probability of failure may be expressed as

$$S_a = A_k \log N + B_k \qquad (6)$$

where S_a=   Stress amplitude
    A_k=   Slope of S-N curve for stress ratio R_{sk}
    N=   Scale parameter for life
    B_k=   Stress amplitude intercept of S-N curve for stress ratio R_{sk}

If the structure's behavior under a fully reversed loading spectrum is being characterized, then there will be three values of A_k and three values of B_k. These constants are readily obtained by a least-squares curve fitting procedure.

Next, the two or three stress ratios that have been characterized using Eq. (6) are plotted on a master diagram. A partial diagram is illustrated in Figure 2 for the case where constant amplitude fatigue test data has been obtained at stress ratios of R_{so}=-1.0, R_{s1}=0.1, and R_{s2}=-10.0. Note that Eq. (6) may be used to determine the fatigue life scale parameter for any arbitrary stress amplitude at the stress ratios tested. For other stress ratios, a modified Goodman relation is used to obtain the fatigue life scale parameters. The general form of this relation is given by

$$S_a = S_{ao} [1 - (\frac{S_{mn}}{R_o})^m] \qquad (7)$$

9

where S_a and S_{mn} are the stress amplitude and mean stress at which the scale parameter for life is desired, respectively, and S_{ao} is the stress amplitude obtained from Eq. (6) for $R_s = R_{so}$. For loadings that fall between the static tension strength and R_{so}, R_o is taken to be the scale parameter for tension strength; otherwise, R_o is taken to be the scale parameter for compression strength. m is a curve-fitting parameter, and is chosen to pass through the appropriate point on the "intermediate" stress ratio line, R_{si}, for which data has been taken. If the Goodman relation is to be between the static tension strength and R_{so}, then $R_{si} = R_{s1}$, and if the Goodman relation is to be between the static compression strength and R_{so}, then $R_{si} = R_{s2}$. To obtain m, let the stress amplitude and mean stress corresponding to the life of interest on the intermediate line be denoted by S_{ai} and S_{mi}, respectively. These values can be obtained from Eq. (6) defined at R_{si}. Then

$$m = \log\left(\frac{1-S_{ai}}{S_{ao}}\right) / \log\left(\frac{S_{mi}}{R_o}\right) \tag{8}$$

Equations (6) - (8) mathematically define a master diagram for life, and the life corresponding to any arbitrary stress amplitude and stress ratio may be obtained by an iterative procedure. For example, for a given S_a and S_{mn} of interest, one "estimates" a corresponding scale parameter for life, N_e. Equation (6) is first applied at R_{so} to obtain the stress amplitude corresponding to N_e. This is denoted in Equations (7) and (8) as S_{ao}. Equation (6) is then applied at R_{si} to obtain the stress amplitude and mean stress corresponding to N_e, denoted in Eq. (8) as S_{ai} and S_{mi}, respectively. These results give m, Eq. (8), and S_a, Eq. (7). If this value of S_a agrees with the value of interest, then the estimate of life was correct. Otherwise, N_e is adjusted and the process repeats until convergence is achieved.

The strength degradation parameter and fatigue life shape parameter are determined from "modified" master diagrams that display lines of constant v or B_1. First, values of v are determined for each stress amplitude and stress ratio at which constant amplitude fatigue tests were performed. This is accomplished using the methodology described in Part I of this work. The resulting values of v are used, as are the previously determined values of B_1, to develop linear S-v and S-B_1 relationships for each stress ratio. This step is essentially the same as was done for the S-N data.
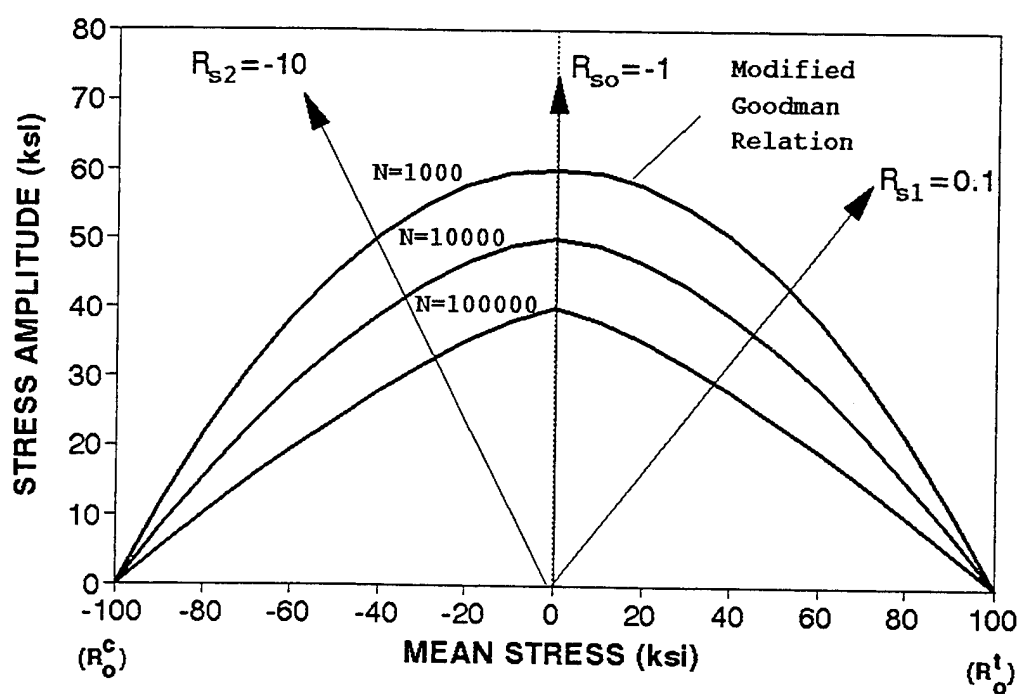
10

Figure 2. Illustration of master diagram with constant life lines of
1000, 10000, and 100000 cycles.

11

Using linear least-squares curve fitting procedures, the constants C_k, D_k, E_k and F_k in the following equations are obtained:

$$S_a = C_k \, v \, + \, D_k \qquad (9)$$

$$S_a = E_k \, B_1 \, + \, F_k \qquad (10)$$

The parameters in Equation (9) and (10) are defined similarly as for Eq. (6); C_k and E_k are the slopes of the curve-fits (corresponding to each stress ratio), and D_k and F_k their intercepts. Master diagrams for v and B_1 are constructed by linearly connecting like values, as depicted in Figures 3 and 4. As for the case for the standard master diagram, the diagrams themselves are primarily for interpretation. Actual values of v and B_1 for a given loading may be found from Equations (9), (10), and an additional pair of equations that provide the slopes of the curves on the modified master diagrams.

3.3 Summary

The procedure for fully characterizing the model for spectrum loading is reviewed below. First, the load spectrum of interest is examined. Of particular importance is the mean stress and stress ratio for each segment in the spectrum. Based on this information, the stress ratios are selected for the experimental database used to characterize the model. Next, the S-N, S-v, and $S-B_1$ relationships are obtained from the constant amplitude fatigue data for each stress ratio. This information is used to generate master diagrams from which the parameters N, v, and B_1 may be calculated for each load segment in the spectrum. Static strength distributions are obtained from monotonic tests, and the cycle mix constants are obtained from large and small block two-stress level fatigue tests. At this point, all model parameters for all load segments in the spectrum are characterized and the model may be applied to predict residual strength and probability of failure.
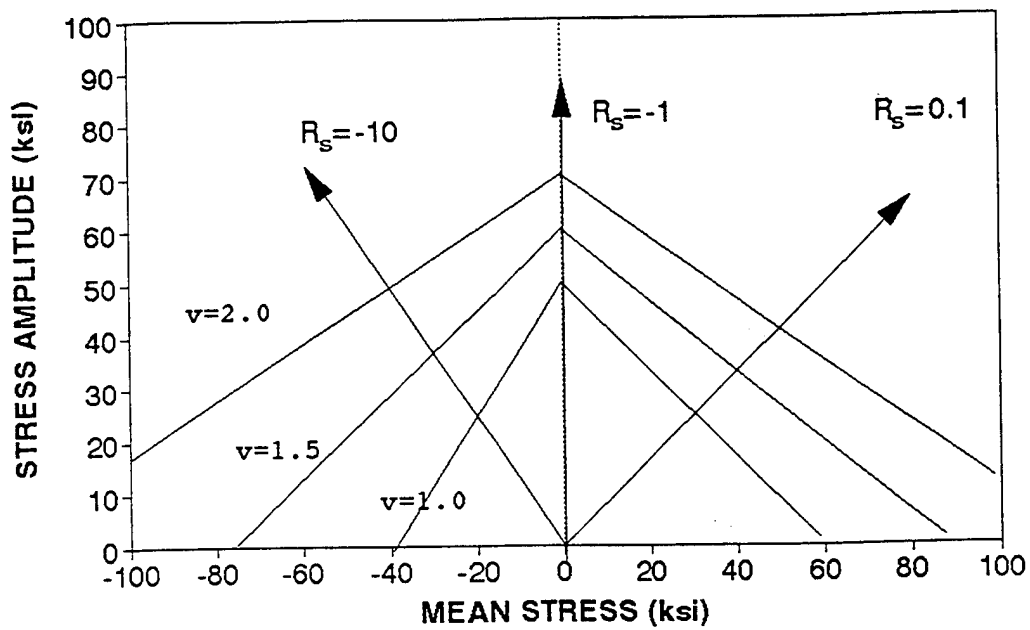
Figure 3. Illustration of modified master diagram for constant v
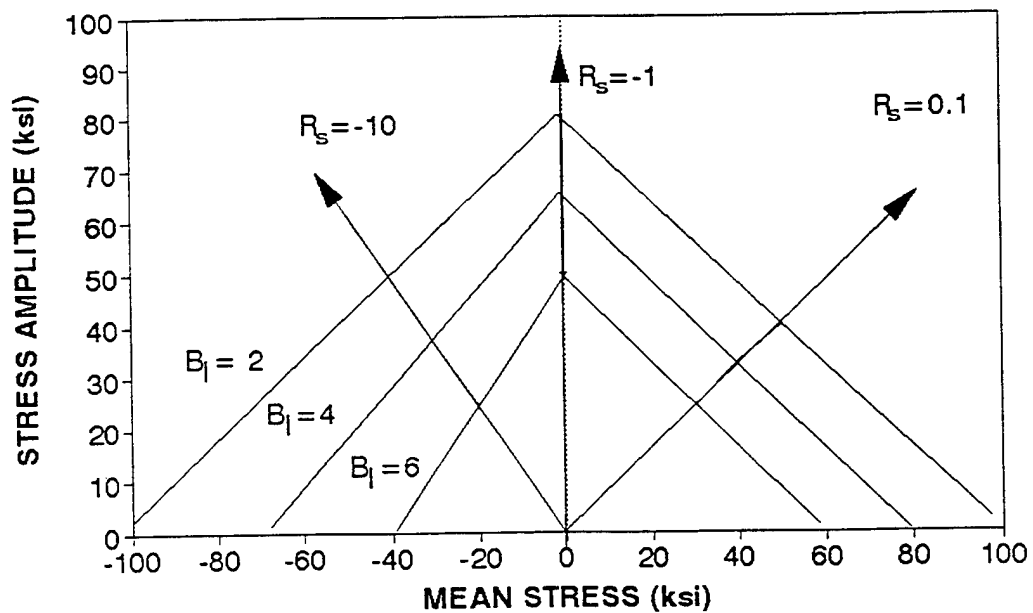lines using data for stress ratios of 0.1, -1, and -10.

Figure 4. Illustration of modified master diagram for constant B_1
lines using data for stress ratios of 0.1, -1, and -10.

13

4. RESULTS

4.1 SGF Spectrum

In this section, life predictions by the model are compared to experimental results reported by Schutz and Gerharz (1977) for uniaxial spectrum loadings of $[0_2/\pm45/0_2/\pm45/\overline{90}]_s$ graphite/epoxy test specimens. All specimens contained a gage section approximately 0.4 inches (10mm) wide by 0.8 inches (20mm) long housed in "Teflon coated anti-buckling supports." Comparisons are made for two Schutz and Gerharz Fighter (SGF) loading spectrums. Each SGF load spectrum simulates the stress history on the upper wing surface at the wing root of a fighter aircraft and consists of a series of 16 compression fatigue loadings of various severities. There are 14,031 cycles in a complete spectrum. This corresponds to approximately 200 flights, or a typical year of service. The loading sequence is such that all loads of a given stress amplitude are applied as a "block."

The individual SGF spectrums are identified by their peak compressive stress. For the test geometries considered, SGF1 contains a peak compressive stress of 105.15 ksi and SGF2 contains a peak compressive stress of 94.56 ksi. Figure 5 presents a bar chart of the magnitudes and sequences of the stresses in the two spectrums. Schutz and Gerharz reported that only three test replicates were performed for each spectrum. Although this is not a statistically significant sampling, we choose to present this data as it has also been used for comparison by Yang (Yang and Du, 1983). We also compare these results to predictions made by Schutz and Gerharz (1977) using the Palmgren-Miner rule (Palmgren, 1924; Miner, 1945).

4.1.1 Model Characterization

The SGF1 and SGF2 spectrums contain only compression dominated loadings. Therefore, according to the recommendations of Table 1, a minimum of 45 tests are required. These include the static compression strength distribution, and the fatigue life distributions for the stress ratios R_{so} and R_{s2}. Both SGF1 and SGF2 contain compression and compression-tension segments, and the largest stress ratio of the compression-tension cycles in either spectrum is approximately -3.75. Schutz and Gerharz generated fatigue life data at three stress ratios: -1.0, -1.66, and -5.0. In what follows, we take $R_{so}= -1.0$ and $R_{s2} = -5.0$ to determine the model's parameters. We also illustrate how the additional data, at $R_s=-1.66$, may be incorporated if so desired. Also, note from Figure 5 that
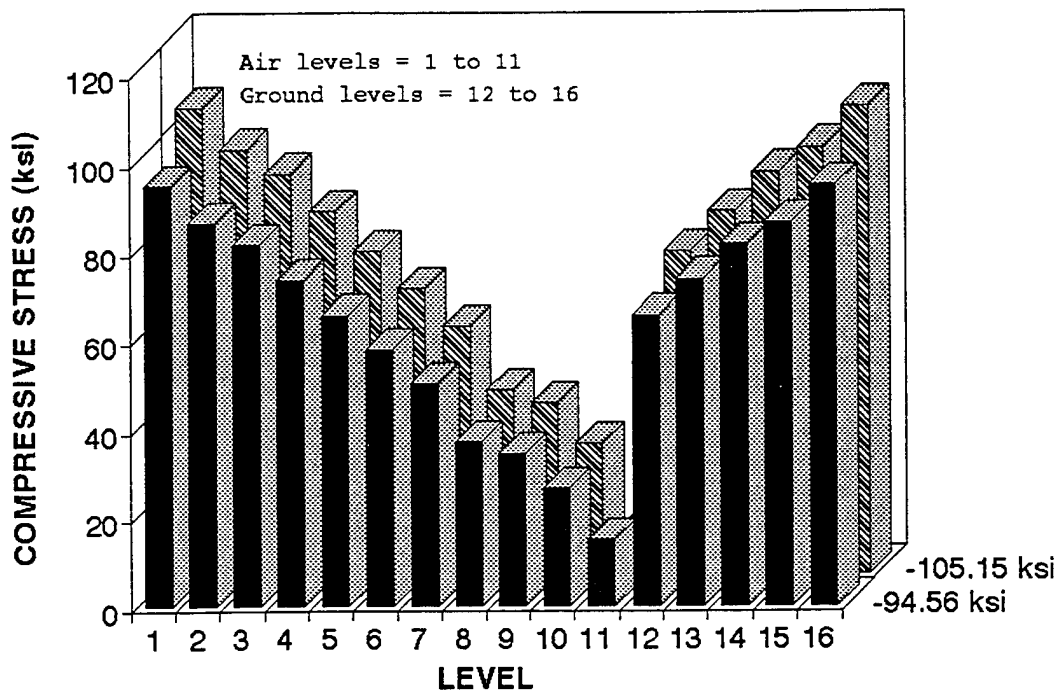
14

Figure 5. Compressive load spectrums used by Schutz and Gerharz (1977) to evaluate spectrum fatigue of graphite/epoxy laminates.

the magnitude of the mean stress decreases for 11 out of the 16 load transitions in the spectrum. As a result of this, along with the fact that the SGF spectrums contain relatively large block loadings, we are able to apply the model without incorporating a cycle mix factor. That is, all predictions for these spectrums use $C_m=0$.

The static compression strength distribution was reported by Schutz and Gerharz (1977) in terms of Weibull parameters. Based on 31 static tests, they obtained $R_o^c=124.0$ ksi and $B_s=28.1$. Data from their constant amplitude fatigue tests was presented graphically, and at least four replicates were performed at each stress amplitude and stress ratio. This data was reduced to obtain N, B_l, and v, and the results are presented in Table 2. Table 3 lists the linear curve fitting constants for the S-N, S-B_l, and S-v curves as defined by Equations (6), (9), and (10).

Table 2. Fatigue Life Distribution Data

R_s	S_a (ksi)	N (cycles)	B_l	v
-1.00	79.2	16,587	4.2	1.20
-1.00	63.6	196,134	5.3	0.90
-1.00	52.7	858,867	5.9	0.50
-1.66	74.0	5,206	4.43	1.70
-1.66	64.0	60,662	6.36	1.50
-1.66	45.5	640,499	2.98	0.75
-5.00	56.0	23,560	2.24	1.60
-5.00	47.1	89,566	4.38	1.50
-5.00	38.1	849,773	4.32	1.00

Table 3. Curve Fitting Constants

R_s	A (ksi)	B (ksi)	C (ksi)	D (ksi)	E (ksi)	F (ksi)
-1.00	-15.4	145	37.3	32.8	-15.5	144
-1.66	-14.8	132	28.6	23.5	4.90	38.6
-5.00	-11.2	104	25.9	11.6	-6.21	69.7

Figure 6 shows the fatigue life master diagrams used to obtain N for SGF1 and SGF2. This figure shows constant life curves for N= 10^3, 10^4, 10^5, 10^6, and 10^7 cycles and was plotted using Equations (6)-(8) and the S-N fatigue

data for R_s=-1 and -5. The figure indicates that R_s=-5 "best characterizes" the loads in the spectrum, and for this reason was chosen as R_{s2}. As discussed previously, the fatigue life scale parameters for any load level may be approximated by interpolation from the figure, however, we used Eqs. (6)-(8) directly. Also, note from Table 2 that none of the experimentally determined constant amplitude fatigue lives extend beyond 10^6 cycles. This data was extrapolated to 10^7 cycles to create the master diagram of Figure 6. Further, note that four load levels in each spectrum fall below the constant life line for N=10^7. To avoid extrapolation beyond 10^7 cycles, we used the conservative estimate that the fatigue lives of these points could be set equal to 10^7 cycles.

Figure 7 shows the modified master diagram for the fatigue life shape parameter, B_1. Linear lines connect like values of B_1 based on the S-B_1 curves for stress ratios of -1 and -5. As in the previous case, 10^7 cycles was used as a "cut-off" value, beyond which we did not extrapolate data. To assist in the determination of B_1 for N>10^7 cycles, the life curve for N=10^7 cycles is also plotted in Figure 7. For load levels below this curve, the fatigue life shape parameter was obtained from the intersection of the N=10^7 curve and the stress ratio of interest. Figure 8 shows the modified master diagram for v. The constant v lines are constructed in this figure by connecting like values of v using *all* the available data, i.e., R_s=-1, -1.66, and -5. Values for v corresponding to R_s=-1.66 are included in Figure 8 primarily to show how additional data may be incorporated. Inclusion of this data does not have a significant affect on predicted lives, nor does choosing R_{so}=-1.66. As in the previous case, N=10^7 was used as a "cut-off" beyond which data was not extrapolated. The model's parameters for SGF1 and SGF2 are listed in Tables 4 and 5, respectively. These values were obtained from Equations (6) - (10) using the previously described procedures.

STRESS AMPLITUDE (ksi)

$R_s = -1$

$R_s = -5$

10^3

10^4

10^5

10^6

10^7

100
90
80
70
60
50
40
30
20
10
0

-130 -120 -110 -100 -90 -80 -70 -60 -50 -40 -30 -20 -10 0

MEAN STRESS (ksi)
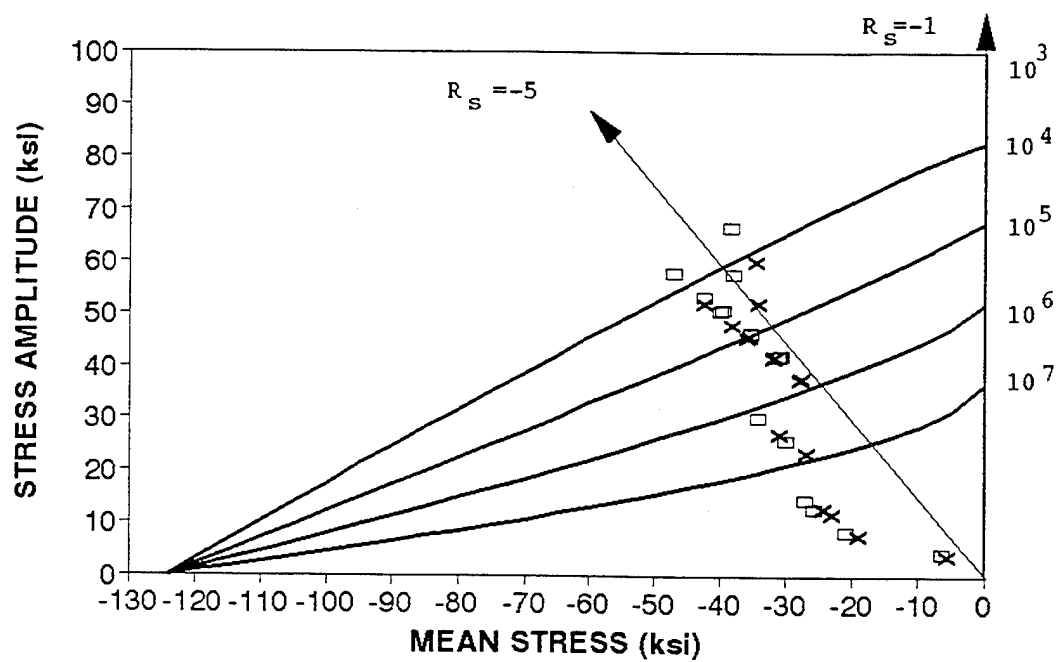
Figure 6. Master diagram for SGF1 and SGF2. The load levels contained in SGF1 are symbolized by an "x" and those in SGF2 are symbolized by a "[]."

18

Figure 7. Modified master diagram for B_l. The load levels contained in SGF1 are represented by an "x." Data used to construct the diagram is indicated by an asterisk.

Figure 8. Modified master diagram for v. The load levels contained in the SGF1 are represented by an "x." Data used to contruct the diagram is indicated by an asterisk.

Table 4. Model Parameters for SGF1

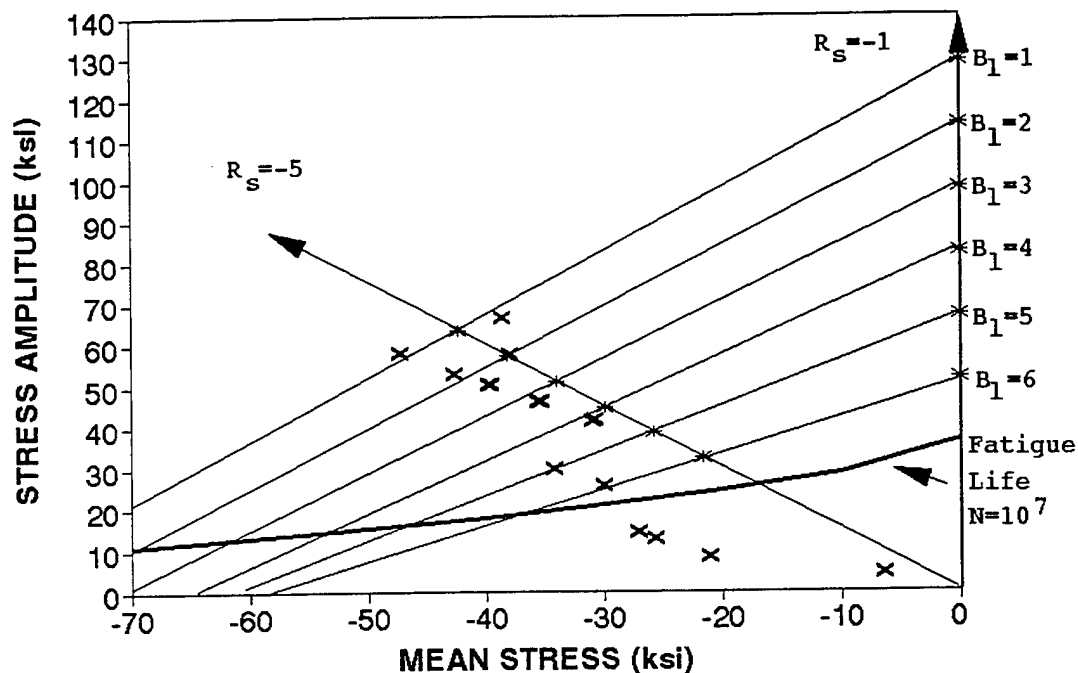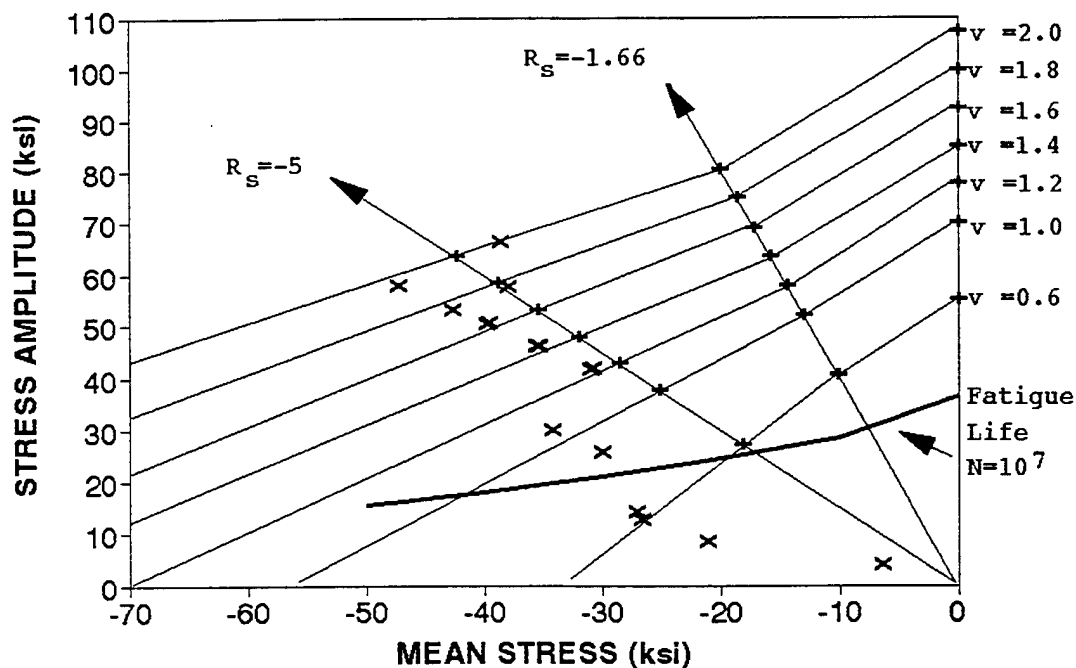| Blk	S_{min} (ksi)	R_s	n	log N	v	B_1
1	-105.15	-3.76	2	3.60	2.00	1.25
2	-95.72	-4.85	7	4.17	1.80	2.00
3	-90.21	-8.20	34	4.55	1.65	2.40
4	-81.65	-7.51	121	5.00	1.40	3.25
5	-72.66	-6.51	290	5.46	1.20	4.15
6	-64.25	15.28	641	6.18	1.20	5.00
7	-55.84	13.28	1136	6.63	1.00	5.90
8	-41.48	3.25	1800	7.00	1.20	6.25
9	-38.43	2.98	2000	7.00	1.00	6.00
10	-29.44	2.33	7000	7.00	1.20	5.50
11	-10.59	4.87	800	7.00	1.00	6.50
12	-72.64	-6.86	100	5.46	1.20	4.25
13	-81.65	-7.71	66	6.04	1.40	3.25
14	-90.35	-8.53	27	4.55	1.60	1.80
15	-95.87	-9.06	5	4.26	1.80	1.75
16	-105.15	-9.93	2	3.77	2.00	1.00

20

Table 5. Model Parameters for SGF2

Level	S_{min} (ksi)	R_s	n	log N	v	B_1
1	-94.56	-3.75	2	4.21	1.75	2.5
2	-86.14	-4.87	7	4.73	1.60	3.0
3	-81.22	-8.24	34	5.08	1.45	3.5
4	-73.35	-7.44	121	5.47	1.25	4.0
5	-65.41	-6.54	290	5.85	1.10	5.0
6	-58.01	15.39	641	6.46	0.95	5.8
7	-50.17	13.31	1136	6.83	0.80	6.5
8	-37.27	3.25	1800	7.00	0.90	6.0
9	-34.66	3.03	2000	7.00	0.95	6.0
10	-26.54	2.32	7000	7.00	1.00	6.0
11	-15.09	5.00	800	7.00	0.80	6.5
12	-65.42	-6.94	100	5.86	1.10	5.0
13	-73.53	-7.80	66	5.47	1.25	4.0
14	-81.35	-8.63	27	5.08	1.40	3.3
15	-86.29	-9.15	5	4.83	1.55	1.8
16	-94.56	-10.05	2	4.39	1.75	2.0

4.1.2 Prediction vs Experiment

Experimental and theoretical fatigue life results are shown in Figure 9 for the SGF1 load spectrum. In the figure, 200 flights corresponds to one time through the spectrum, e.g., the 14,031 cycles comprising the 16 load levels depicted in Figure 5. For this loading, the model demonstrates good correlation with experiment and provides somewhat better agreement than Yang's model. The Palmgren-Miner rule predicted the mean fatigue life, or 50th percentile, to be 28,490 flights. This is more than 3 times larger than the observed value.

Figure 10 compares the model's predictions with experiment, and with predictions by Yang's model for SGF2. Again, the best predictions are obtained using the present approach. The Palmgren-Miner rule predicted a mean fatigue life of 90,090 flights; this exceeded the experimental results by a factor of four.
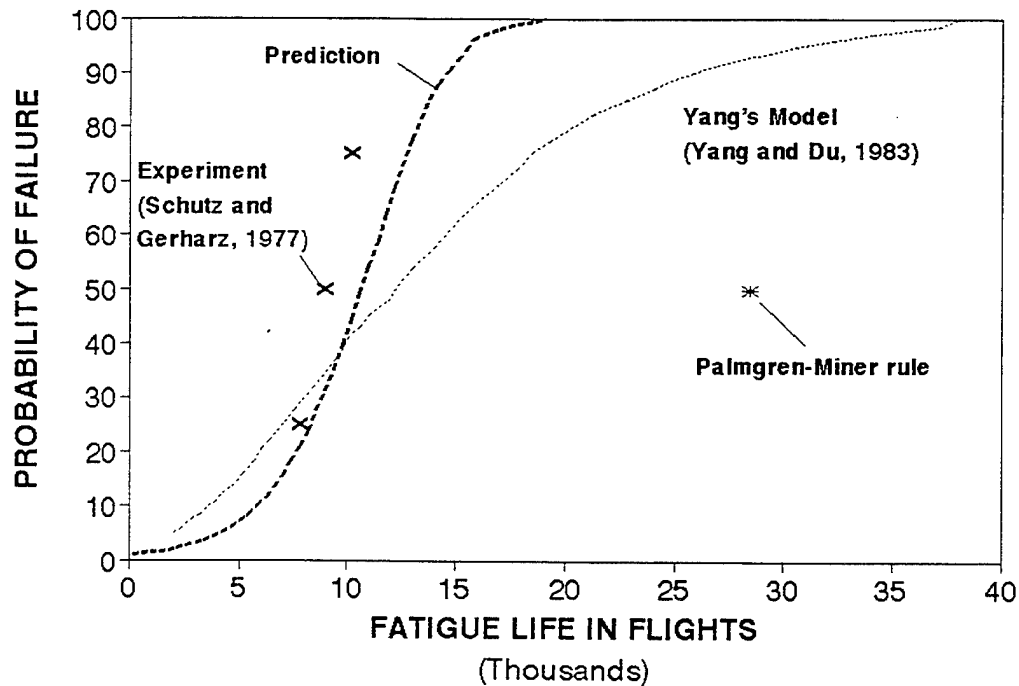
Figure 9. Comparison of prediction to Yang's model, the Palmgren-Miner rule, and to experiment for SGF1.
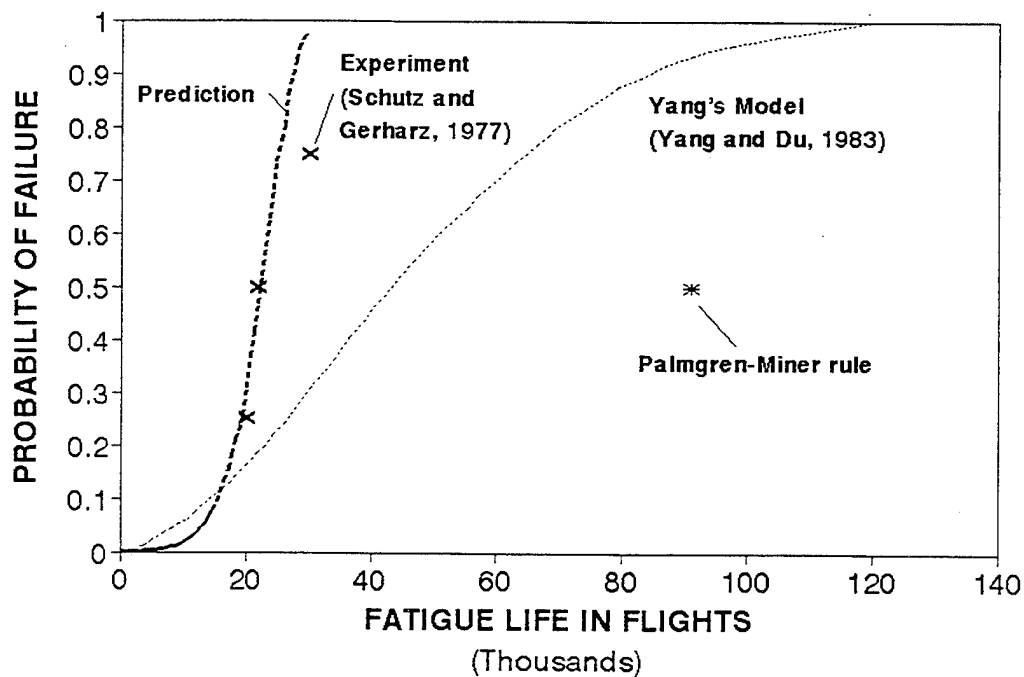

Figure 10. Comparison of prediction to Yang's model, the Palmgren-Miner rule, and to experiment for SGF2.

4.2 FALSTAFF Spectrum

In this section, life predictions by the model are compared to experimentally obtained fatigue life distributions for graphite/epoxy laminates subjected to the Fighter Aircraft Loading STAndard For Fatigue (FALSTAFF) spectrum. These results were obtained from the FAtigue and Damage tolerance Data (FADD) test program conducted by Farrow (1989). Two types of laminates were considered: 1) a predominately angle-ply XAS/914C graphite/epoxy laminate, with an orientation of $[\pm45/90/(\pm45)_4]_s$ (hereafter referred to as "angle-ply"), and 2) a quasi-isotropic XAS/914C graphite/epoxy laminate, with an orientation of $[\pm45/0/90]_{3s}$. All tests consisted of uniaxially loaded, 10.6in (270mm) long x 1.18in (30mm) wide, "fastener type" specimens. These specimens contained a 0.19in (4.83mm) diameter drilled and countersunk hole, into which a 0.19in (4.81mm) diameter countersunk fastener was placed and torqued to 6.78ft-lb (5.0 Nm). All data from the FADD study was reported by Farrow in the form of Weibull distributions; it is stated that Weibull scale and shape parameters were calculated using the maximum likelihood technique (Talreja, 1981) and a minimum of six data points. All reported stresses are based on "net section area," i.e., the specimen width, less the hole diameter, multiplied by the thickness.

4.2.1 Introduction to FALSTAFF

FALSTAFF is a standardized random-ordered loading spectrum that simulates the in-flight load-time history of fighter aircraft. One spectrum "block" contains a series of 17,983 cycles which simulate the loading on the wing skin of a fighter aircraft over a period of 200 flights (Van Dijk and De Jonge, 1975; Have, 1989). The loading sequence is different for each flight, and depends on the type of aircraft, the take-off weight, and the aircraft's mission. The magnitude and sign of each individual load level is directly proportional to a user defined test limit stress, S_L, which may be positive or negative. The flexibility of the FALSTAFF spectrum allows a wide variety of very different loading spectrums to be defined. As such, the FALSTAFF spectrum is commonly used in the production of fatigue life and/or crack growth data.

4.2.2 Model Characterization for FALSTAFF

Characterization of the model for the FALSTAFF spectrums is essentially the same as outlined for the SGF1 and SGF2 spectrums. The two fundamental differences are that (1) characterization testing is performed at three stress ratios, $R_{s1}=0.1$, $R_{so}=-1.0$ and $R_{s2}=10.0$, and (2) a cycle mix constant is often required. The cycle mix effect may be important in the FALSTAFF spectrum, as many of the constant amplitude segments are only a few cycles in length. A detailed description of the characterization procedure for both laminate types is presented in Schaff and Davidson (1994b).

4.2.3 Prediction Versus Experiment for Angle-Ply Laminates

The experimental data on the angle-ply laminates was compared to the model's predictions for FALSTAFF load spectrums containing test limit stresses of 30.3, 25.9, -37.7 and -33.1 ksi. For reference, the static strength scale parameters for these laminates were 36.3 ksi for tension and -44.0 ksi for compression. The model's predictions that are presented in this section used $C_m=5.38 \times 10^{-7}$; this value was determined according to the procedure in Part I (Schaff and Davidson, 1994a) and specifics are given in Schaff and Davidson (1994b). Although the value of C_m was determined from tension-tension loading, it was used for both tension and compression dominated FALSTAFF spectrums. This was necessary simply because sufficient data was not presented by Farrow (1989) to determine C_m for transitions to a negative mean stress. In order to demonstrate the affect of the cycle mix factor on the predicted life distributions, the "fatigue life," used subsequently to denote the 63.2 percentile of the failure distributions, is presented for both $C_m=0$ and for $C_m=5.38 \times 10^{-7}$.

Figure 11 shows the probability of failure as predicted by the model and as obtained by experiment for a test limit stress of 30.3 ksi. For this load case, the model's predictions show excellent correlation to experiment. The theoretical and experimental failure curves agree within 5% throughout the entire range of failure probability values. For the "fatigue life," hereafter used without quotes to refer to the 63.2 percentile of the distribution, the model's prediction and the observed results are 31 and 29 blocks respectively. For comparison, if cycle mix is neglected in the wearout model (i.e., $C_m=0$), the model over-predicts the fatigue life by a factor of two. Thus, by accounting for cycle mix, the predictive capability of the model is significantly improved. For the same load case, the Palmgren-Miner rule
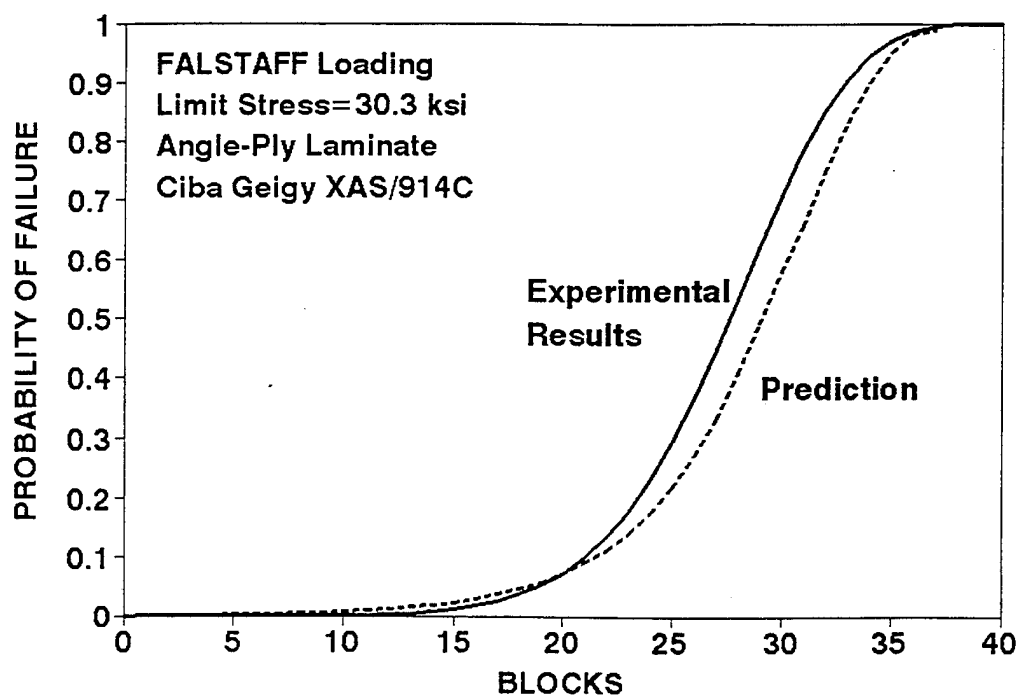
Figure 11. Comparison of predicted and observed results for a
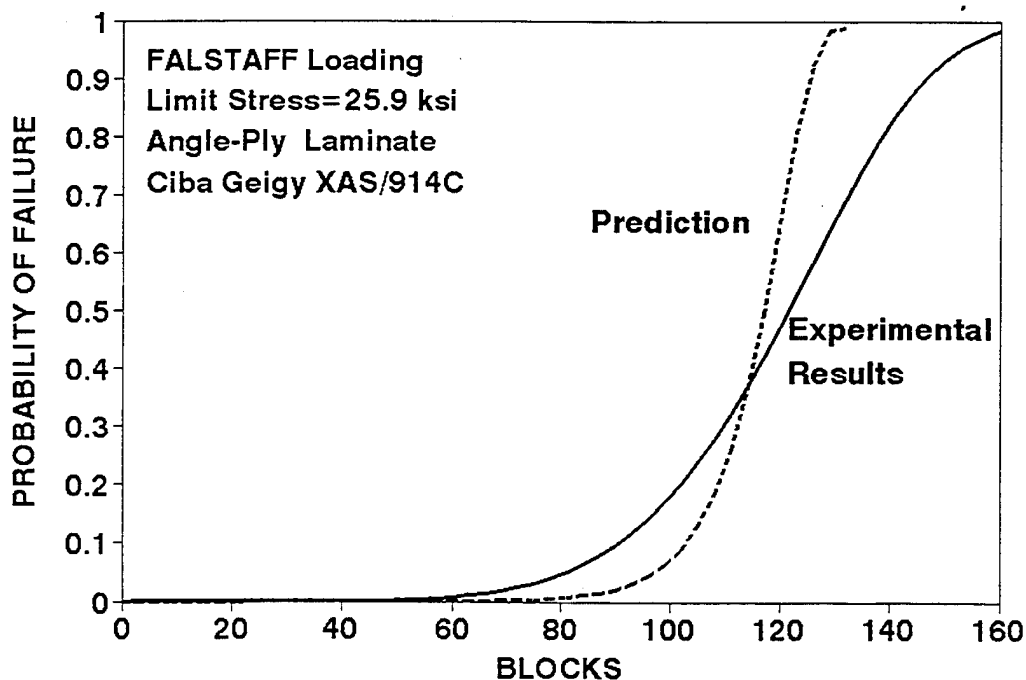FALSTAFF loading with a limit stress of 30.3 ksi
(data of Farrow, 1989)

Figure 12. Comparison of predicted and observed results for a
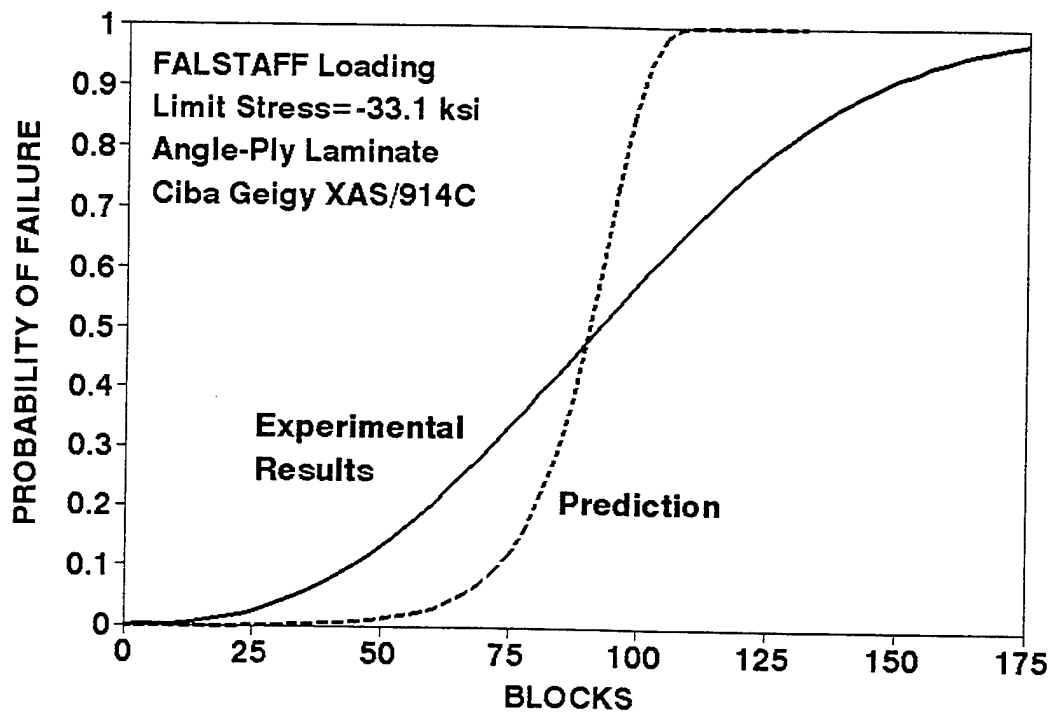FALSTAFF loading with a limit stress of 25.9 ksi (data of Farrow, 1989)

Figure 13. Comparison of predicted and observed results for a
FALSTAFF loading with a limit stress of -33.1 ksi (data of Farrow, 1989)

predicted the mean fatigue life, or 50th percentile, to be 185 blocks. This exceeds the experimental mean of 28 blocks by over a factor of six.

The FALSTAFF load case defined by a 25.9 ksi test limit stress is presented in Figure 12. In this figure, reasonable correlation is obtained for the failure distributions. The model's predictions for fatigue life are within 5% of the experimental results. As in the previous case, the predictions from the model without the cycle mix factor, and by the Palmgren-Miner rule, provided unconservative estimates of fatigue life.

Figure 13 shows the results for a compression load case on the angle-ply laminate with a test limit stress of -33.1 ksi. Relatively good correlation is once again observed, although the predicted distribution is not quite as disperse as the experimental results. Further discussion of the reasons for this are presented in Schaff and Davidson (1994b), as are observed versus predicted life distributions for S_L=-37.7 ksi.

4.2.4 Prediction Versus Experiment for Quasi-isotropic Laminates

Figures 14 and 15 present the model's predicted probability of failure versus the experimental fatigue life distributions for quasi-isotropic laminates subjected to FALSTAFF spectrums with test limit stresses of -69.4 ksi and -65.5 ksi, respectively. The static strength scale parameter for compression for this laminate equals -78.4 ksi. The model's results presented in this section do not account for cycle mix effects. This was due to the absence of the two-stress level fatigue data that is necessary to determine the cycle mix constant. However, based on the damage mechanisms involved, one would expect the cycle mix effect to be less important in quasi-isotropic than in angle-ply laminates and in general, less important for increasingly fiber dominated layups. Indeed, the wearout model without the cycle mix factor agrees reasonably well with the experimental data for both load spectrums. For the data of Figure 14, the model under-predicts fatigue life by 10%; for comparison, the Palmgren-Miner rule predicts the average fatigue life to be 913 blocks, whereas the experimental value was 75 blocks. In Figure 15, the wearout model over-predicts the experimental fatigue life by 38%. The under-prediction of life for the spectrum of Figure 14, and the over-prediction of life for that of Figure 15, suggests that the degradation of strength and fatigue life due to cycle mix effects are not significant for the quasi-isotropic laminate in compression dominated loadings. Further testing is required to ascertain whether this result can be extended to other materials and load spectrums.
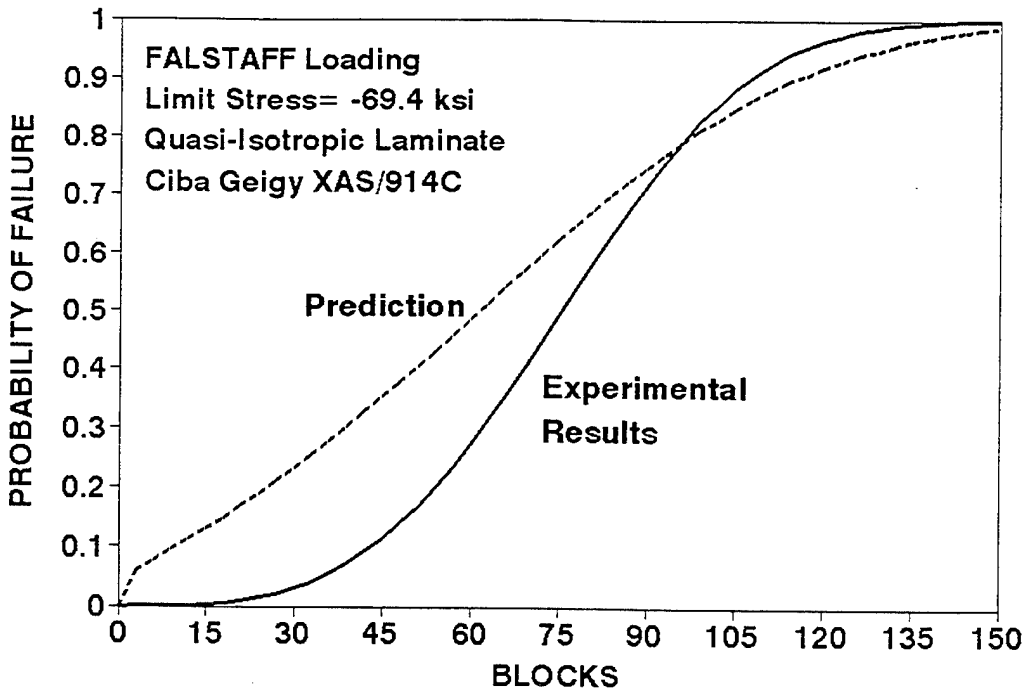
Figure 14. Comparison of predicted and observed results for a
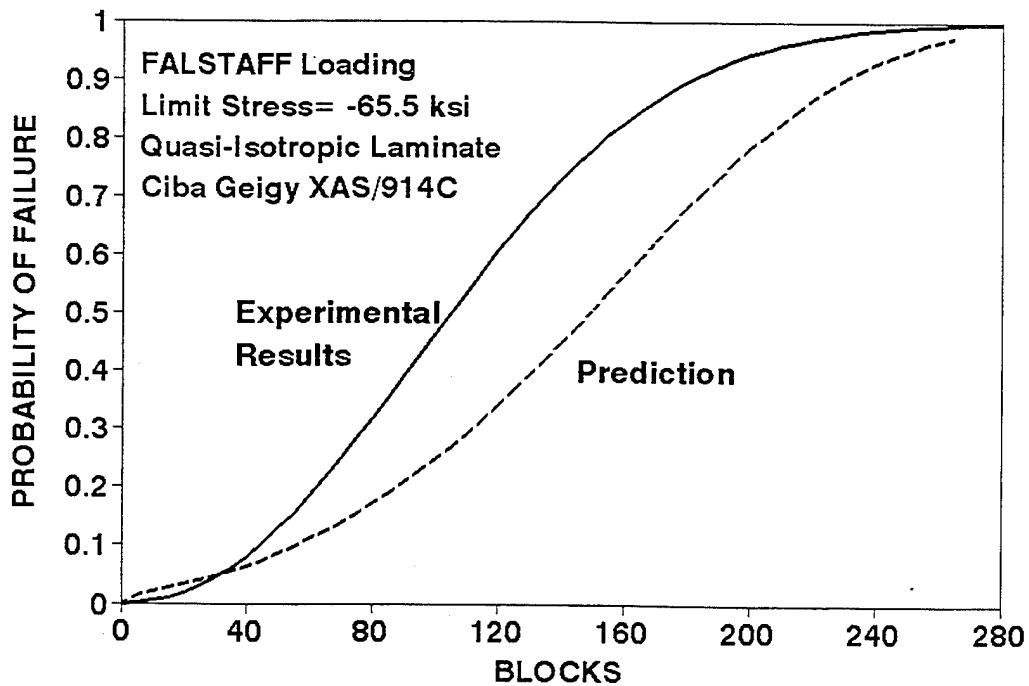FALSTAFF loading with a limit stress of -69.4 ksi (data of Farrow, 1989).

Figure 15. Comparison of predicted and observed results for a
FALSTAFF loading with a limit stress of -65.5 ksi (data of Farrow, 1989).

Table 6 summarizes the results for all laminates subjected to FALSTAFF loadings that we have considered to-date. Results are presented for fatigue life, e.g., for the 63.2 percentile of the predicted life distribution, both with ($C_m \neq 0$) and without ($C_m = 0$) inclusion of the cycle mix effect. In all cases, the model's fatigue life predictions with the cycle mix factor incorporated are quite good. This is particularly impressive considering the complexity of the loading and the relative simplicity of the model. In all cases, the Palmgren-Miner rule, which predicts the 50th percentile of the life distribution, is highly unconservative. Also, for all cases considered to-date, this model shows better correlation to experiment than all other fatigue models of which we are aware.

Table 6. Fatigue Life Prediction Comparisons (FALSTAFF blocks to failure)

Limit Stress (ksi)	Laminate type	Model $C_m=0$ (63.2%)	Model $C_m \neq 0$ (63.2%)	Observed Fatigue Life (63.2%)	P-M Prediction (50%)	Observed Fatigue Life (50%)
30.3	angle-ply	59	31	29	185	28
25.9	angle-ply	236	120	129	790	122
-37.7	angle-ply	53	26	38	240	36
-33.1	angle-ply	251	94	106	790	92
-69.4	quasi-iso	76	NA	84	913	75
-65.5	quasi-iso	171	NA	124	1291	104

5. CONCLUSION

A residual strength-based wearout model has been presented for the life prediction of composite structures subjected to complex spectrum fatigue loadings. Similar to those developed previously, this model is phenomenonolgical and semi-empirical. However, only a limited experimental database is required for model characterization. Most importantly, the model has shown excellent correlation to a variety of experimental results, including highly complex FALSTAFF loading spectrums. This is particularly true if fatigue life comparisons are based on the 63.2 percentile of the probability of failure distribution.

In terms of its predictive capability, the model herein is the most successful, of which the authors' are aware, for

life assessment of composite laminates subjected to spectrum fatigue loadings. In an effort to further increase the model's accuracy, we are currently performing a more comprehensive investigation of the effects of cycle mix. We are also evaluating various modifications to the model to obtain better predictions for fatigue life for the lower end of the probability of failure curves, i.e., in order to predict a statistically significant "minimum life." However, it is our belief that the current model is sufficiently accurate to be incorporated into the present day design process, thereby providing more efficient utilization of composite materials in the development of new composite structures. Incorporating model characterization into the design process will also offer significant benefit for cases where it is found that the loading spectra are different than those used for the structure's design. That is, rather than embarking on expensive test programs, this model may be used to determine an updated life based upon the true service usage.

6. BIBLIOGRAPHY

Farrow, I. R., 1989, "Damage Accumulation and Degradation of Composite Laminates Under Aircraft Service Loading: Assessment and Prediction Vol. I and II," Cranfield Institute of Technology, Ph.D. Thesis.

Goodman, J., 1930, Mechanics Applied to Engineering, Vol. 1, 9th Ed., Longmans Green, London.

Hahn, H. T., 1979, "Fatigue Behavior and Life Prediction of Composite Laminates," Composite Materials, Testing and Design (Fifth Conference), American Society for Testing Materials, STP 674, S.W. Tsai, Ed., pp. 383-417.

Have, A. A., 1989, "European Approaches in Standard Spectrum Development," American Society for Testing and Materials, STP 1006, pp. 17-35.

Miner, M.A., 1945, "Cumulative Damage in Fatigue," Journal of Applied Mechanics, Vol. 12, pp. 159-164.

Palmgren, A., 1924, "Die Lebensdauer von Kugellagern," Zeitschrift des Vereins Deutscher Ingenieure, Vol. 68, pp. 339-341.

Schaff, J. R. and Davidson, B. D., 1994a, "Life Prediction Methodology for Composite Laminates. Part I: Constant Amplitude and Two-Stress Level Fatigue," WL-TR-94-4046, Air Force Wright Laboratory.

Schaff, J. R. and Davidson, B. D., 1994b, "Life Prediction for Composite Laminates Subjected to Spectrum Fatigue Loading, Durability of Composite Materials, R.C.Wetherhold, Ed., The American Society of Mechanical Engineers, MD-Vol. 51, pp. 90-109.

Schutz, D. and Gerharz, J.J., 1977, "Fatigue Strength of a Fibre-Reinforced Material," Composites, Vol 8, No. 4, pp 245-50.

Talreja, R., 1981, "Estimation of Weibull Parameters for Composite Materials Strength and Fatigue Life Data," Fatigue of Fibrous Composite Materials, American Society for Testing Materials, STP 723, pp. 291-311.

Tsai, S. W., 1988, "Composites Design," 4th Edition, Think Composites, Dayton, Ohio.

Van Dijk, G.M. and de Jonge, J.B., 1975, "Introduction to FALSTAFF," Proceedings 8th ICAF Symposium, ICAF Document No. 801.

Yang, J. N. and Du, S., 1983, "An Exploratory Study Into the Fatigue of Composites Under Spectrum Loading," Journal of Composite Materials, Vol. 17, pp. 511-26.